JOURNAL OF MATERIALS SCIENCE **38** (2003) 165–171

The tensile deformation of flax fibres as studied by X-ray scattering

O. M. ASTLEY, A. M. DONALD*
Polymers and Colloids Group, Cavendish Laboratory, Madingley Road, Cambridge CB3 0HE, UK
E-mail: amd3@phy.cam.ac.uk

Small and wide-angle X-ray scattering experiments with *in-situ* deformation of dry flax fibres have been carried out. An increase in the (200) peak intensity during deformation has been attributed to strain-induced crystallisation of the cellulose microfibrils, and provides evidence that the non-crystalline cellulose chains are initially oriented. However, no change in the equatorial small-angle streak (from cellulose microfibrils), the meridional reflection (from a crystalline/non-crystalline repeat along the fibre), or the microfibril orientation was seen.

1. Introduction

Plant cells are surrounded by a cell wall that consists of cellulose microfibrils in a biopolymer matrix of pectins, hemicelluloses and proteins [1]. The wall is made up of three layers (Fig. 1). The primary wall is the outermost layer that grows as the cell does. The secondary wall is formed inside the primary wall once the cell has stopped growing. At the inner-most level is the plasma membrane, a lipid bilayer. The cellulose in plant cells is almost exclusively in the crystal form cellulose I, with conversion to cellulose II possible by chemical treatment [2].

The work that will be discussed here has concentrated on studying the properties of the secondary cell wall, the wall that is important during food harvesting and processing, and is used to make paper and textiles. The results may also yield information which can explain the behaviour seen in primary walls, since although much work has been directed at the structure and enlargement of the primary cell walls of growing plants [3–6], it is still unclear how this occurs.

In a previous paper [7] we have described small-angle X-ray scattering experiments on flax fibres under different hydration conditions. This paper will extend that work to consider the effect of tensile deformation on both the small-angle and wide-angle scattering patterns.

Flax (*Linum usitatissimum*) is a useful material for investigating the plant cell wall, as the fibres have a thickened secondary wall with enough material to scatter X-rays from a small number of fibres. It is therefore not necessary to average over a large fibre bundle. In addition, the fibres have a proportion of non-cellulosic materials that is more representative of plant cell walls in general than certain other fibres, such as cotton, that are almost 100% cellulose [8]. The flax fibres are made up from single sclerenchyma cells, the so-called elementary fibres. These are joined together by a pectin interface into technical fibres which are 50–100 μm in diameter. The technical fibre bundles are separated from each other by partial decomposition of the cell wall by bacteria (retting) and then by beating and combing (scutching and hackling) [9].

We have concentrated on the use of X-ray scattering and *in-situ* tensile deformation experiments. X-ray scattering allows the material to be studied in its natural state. Tension experiments are a basic experimental technique to probe the strength of materials, because although they do not mimic well the types of stress that the cell wall is typically put under (for example due to environmental effects or harvesting), the experiments are easy to perform and the results easy to interpret.

2. Materials and methods

Flax fibres from Cebeco, The Netherlands, were kindly provided by the Agrotechnological Research Institute (ATO-DLO), Wageningen, The Netherlands. The fibres had been extracted by warm water retting and then the technical fibres removed by laboratory scale hackling.

Uniaxial tension experiments were performed under constant extension conditions of between 0.01 mm/min and 10 mm/min using a Polymer Laboratories Minimat and a tensiometer built at the Cavendish Laboratory. The Cavendish tensiometer allowed samples to be stretched from both directions, so keeping the same part of the sample in the X-ray beam, unlike the Minimat which only pulled from one direction. The results from both machines were similar.

Load-extension curves are shown here instead of stress-strain curves because of the difficulty in measuring the sample cross-section due to the variable number of elementary fibres in a technical fibre and so in the sample, and the small cross-section of the elementary fibres (10–25 μm diameter).

*Author to whom all correspondence should be addressed.

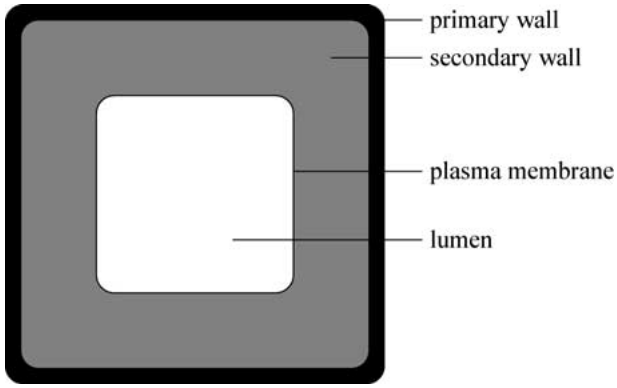

Figure 1 A schematic of the structure of the plant cell wall showing the cell wall layers and the lumen (cell contents).

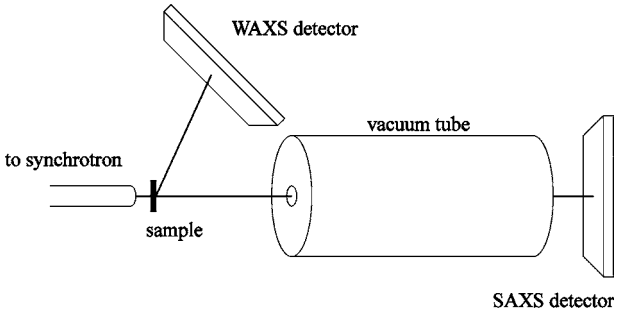

Figure 2 A schematic of the setup for simultaneous small and wide-angle scattering experiments. Note the unusual positioning of the wide-angle detector, not perpendicular to the X-ray beam.

In-situ uniaxial tension and time-resolved small-angle (SAXS) and wide-angle (WAXS) X-ray scattering experiments were performed at the Daresbury synchrotron source on the non-crystalline diffraction stations 2.1 and 16.1. The data was collected with two-dimensional gas-filled area detectors with 512×512 pixels. In the small-angle experiments a camera length of approximately 3 m was used giving a q range of $0.011\ \text{Å}^{-1} < q < 0.20\ \text{Å}^{-1}$. The experimental setup for simultaneous experiments is shown in Fig. 2. It was not always possible to get a suitable q range with both detectors because if the WAXS detector was low enough to accept the first few cellulose peaks, the bottom of the detector would interfere with the tail of the SAXS scatter. For this reason the results shown here will be from separate SAXS and WAXS experiments.

The use of intense synchrotron radiation allows scattering from a small number of flax fibres to be measured, allowing a better estimate of the properties of a single cell wall than averaging over a large fibre bundle. In order to collect sufficient data, extension rates of 0.01–0.1 mm/min were used and data collected in time frames of 2 min (SAXS) and 10 min (WAXS).

Because of these long data collection times it was not possible to stretch the flax fibres in a completely hydrated state since dehydration would occur during data collection. For this reason only data from dry fibres is shown, even though it is known that the scattering from fibres changes depending on the hydration level [7, 10], and that the load-extension curves also change (unpublished data and reference [11]).

Before processing, the data was corrected for detector abnormalities by dividing the data by a detector response, and for background air scatter by subtracting a blank scattering pattern. The background subtraction was particularly important for the wide-angle data, where air scatter was as intense as sample scatter. Normalisation to the beam intensity was performed by integrating the total intensity scattering into a corner of the detector well away from any cellulose scattering (SAXS or WAXS), and then dividing the data by this value.

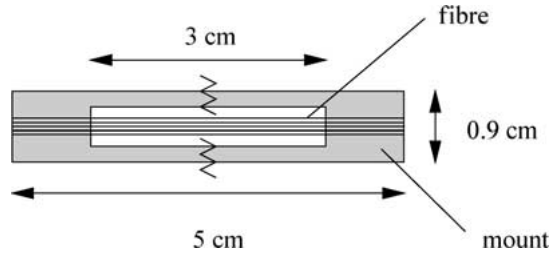

Figure 3 The cardboard mount (shaded) used for the flax fibres for X-ray scattering experiments at Daresbury and the uniaxial tension experiments performed. The flax fibres were attached to the mount with Araldite. The supports were cut before stretching.

To position the fibres in the beam, approximately five to ten aligned technical fibres were aligned, lightly stressed at each end with a small bulldog clip (weighing 6 g each), and glued onto a cardboard mount with Araldite. The resulting sample is shown in Fig. 3. The unstretched fibre length was 20 mm or 30 mm.

3. Results and discussion

3.1. Uniaxial tension

Fig. 4 shows typical load-extension curves for dry flax fibres. This graph illustrates the range of break points due to differences between samples in the degree of damage (which changes the breaking load and extension) and to differences in the cross-section since we are plotting the load-extension and not stress-strain graph. This wide variability has also been found in other cellulose I fibres [11, 12].

The load-extension curve shapes for dry fibres were found to be similar over the range of extension rates 0.01–10 mm/min. Deformation was entirely elastic until fracture and no plastic region occurred unlike in cellulose II fibres [13, 14].

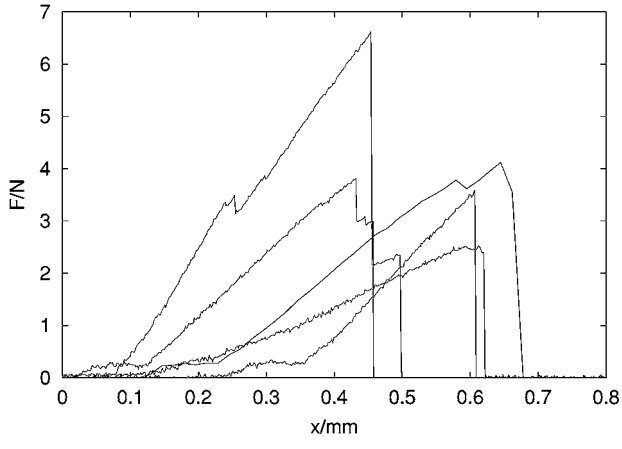

Figure 4 Load-extension curves showing the variable behaviour of flax fibres under strain. All of these samples were bundles of a few (∼5) technical flax fibres in the dry state, strained at a constant 0.01 mm/min. Sample initial length 20 mm.

3.2. Small-angle scattering

Fig. 5a shows a typical small-angle two-dimensional scattering pattern from cellulose fibres. The equatorial (vertical) streak is attributed to the cellulose microfibrils [10, 15]. Also present are meridional (horizontal) spots which we have attributed to a crystalline/non-crystalline repeat length along the fibre of 60–70 Å [7].

In order to determine if the structure of the flax fibres changed on the small-angle length scale, three measurements were made. The equatorial intensity, $\tilde{I}(q)$, was measured by integrating the intensity scattered into a long horizontal rectangle of height 1 pixel, as shown in Fig. 5b. This approach is equivalent to slit-smeared radiation from an infinite slit [16]. The meridional intensity, $I(q)$, was found by integrating over a rectangle of height 39 pixels (the beamstop height) and width 1 pixel, as shown in Fig. 5b. The azimuthal intensity $I(\phi)$ at constant scattering vector q was also measured. Neither the equatorial nor the meridional scattered intensity showed measurable changes during stretching. As we have previously discussed [7], the fibres need to be in the wet state before analysis techniques such as Guinier or Porod [17] can be used on SAXS curves because then the fibre has swollen sufficiently that inter-particle interference effects between the cellulose microfibrils can be ignored. Therefore no length scale information could be extracted from the equatorial intensity curves since these fibres were dry. As regards the meridional scattering, no change in any of the peak position, intensity, or curve shape was seen, although previous studies have shown that the long period in synthetic fibres, attributed to lamellar stacks along the fibres, can increase on stretching in nylon 6 [18–20], in poly(vinylidene fluoride) [21], and in a poly(ether ester) copolymer [22]. However in some cases, such as poly(*p*-phenylene benzobisoxazole) (PBO) no change in long period but a change in intensity was noticed [23].

One explanation for the lack of any change of meridional intensity in the flax fibres would be that the non-crystalline regions between the crystallites are strained initially and therefore cannot stretch without breaking. Such a situation is shown in Fig. 6 for a repeat

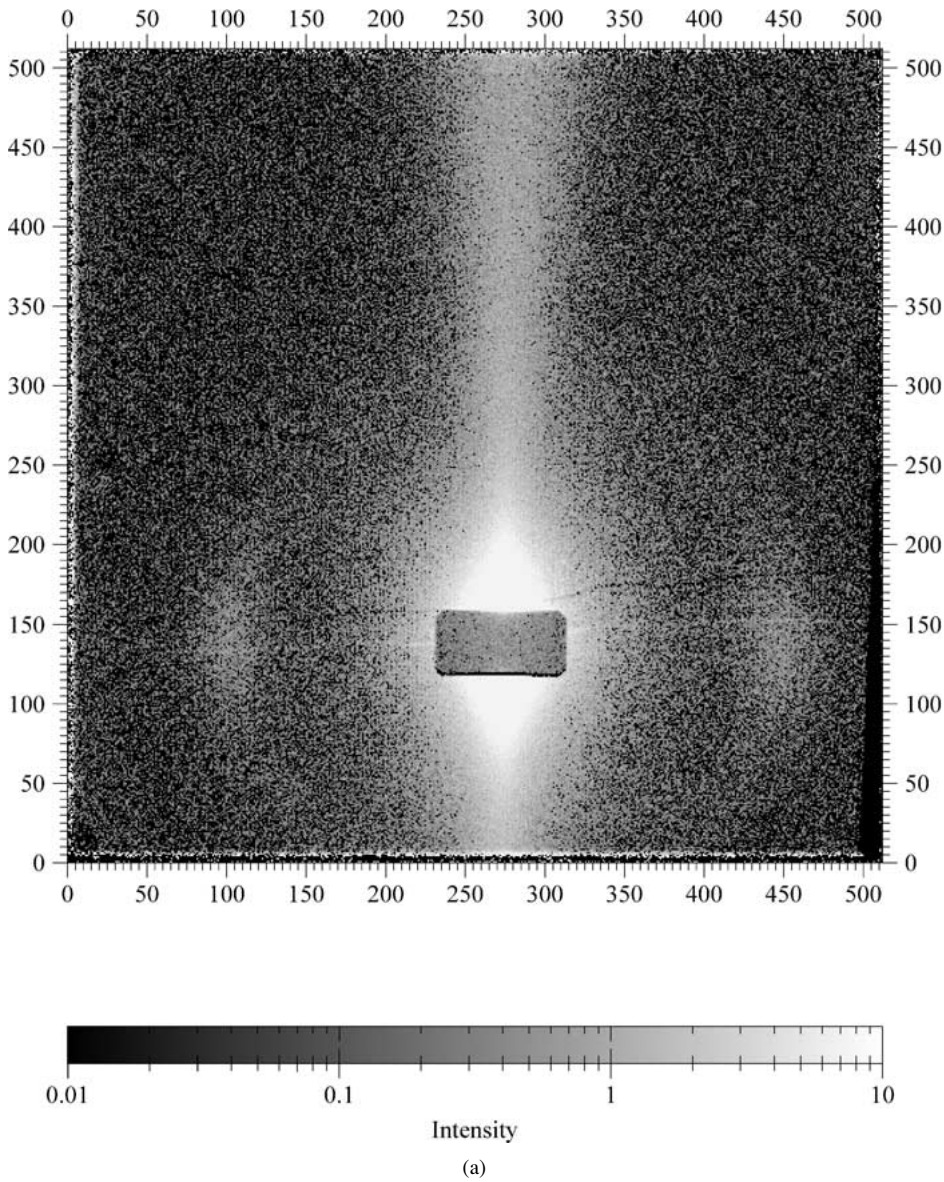

(a)

Figure 5a (a) A typical small-angle diffraction pattern from horizontal dry flax fibres, recorded at $\lambda = 1.4$ Å with a camera length of approximately 3 m and exposed for 2 min. (b) The schematic scattering pattern, together with the areas that are summed over to find the scattering intensity in the equatorial (e) and meridional (m) directions, $\tilde{I}(q)$ and $I(q)$ respectively. (*Continued*.)

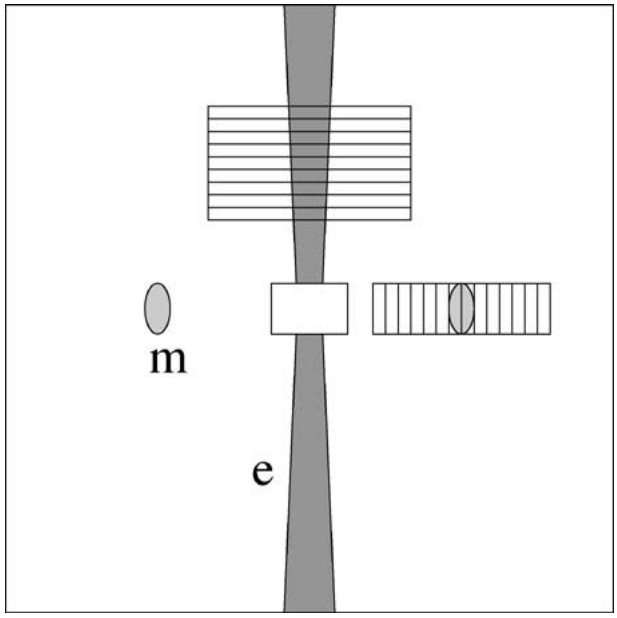

(b)

Figure 5b (*Continued*).

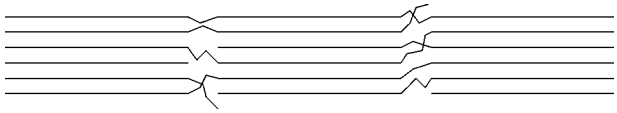

Figure 6 The non-crystalline regions that might exist in flax with a crystal length of 60 Å and a crystal + non-crystalline repeat length of 70 Å. In (a) the long period would be expected to increase on stretching since the molecules in the non-crystalline regions are not taut, but in (b) this would not be expected. In practice no change in long period was seen, suggesting that (b) is the situation in flax.

length of 70 Å and a crystal length of 60 Å. The crystal length used was arbitrary, but must be large enough that the material would count as crystalline and not non-crystalline. Such a situation also agrees with the very limited observed maximum strain of $\epsilon_{\max} \sim 0.05$ (that is 5% extension for fibres of starting length 20 mm as used here): if the molecules in the non-crystalline region were not already stretched the crystals could separate further and $\epsilon_{\max}$ would be larger. This interpretation also agrees with the form of the load-extension curve that the deformation is only elastic and shows no plastic yield point. However it is clear that the data presented cannot unambiguously confirm this interpretation.

3.2.1. Azimuthal SAXS

It is also possible to measure the azimuthal scattered intensity $I(\phi)$. Theory predicts that if the small-angle scattering is from long rods with length l_3 and a Gaussian misorientation defined by the standard deviation σ, then

$$(qB)^2 \approx \frac{\pi}{\ln 2}\frac{4b^2}{l_3^2} + 2\pi\sigma^2 q^2, \qquad (1)$$

where B is the integral breadth of the (Gaussian) curve $I(\phi)$, and $b \approx 1.3916$ [7].

We have already shown that a graph of $(qB)^2$ against q^2 changes during dehydration [7], but it appears that no changes in this curve occur during deformation. Due to the noisy behaviour of the curve for dry fibres this curve is not reproduced here. Azimuthal scattering curves, $I(\phi)$, at different values of q and different time frames also show that there are no orientational changes (either full width at half maximum or mean direction) of the cellulose microfibrils within the limits of accuracy of the measurement.

3.3. Wide-angle scattering

Although no changes are seen in the small-angle scattering curves as the flax fibres are stretched, several changes are seen in the wide-angle regime.

Fig. 7 shows a typical wide-angle scattering pattern from the flax fibres on a two-dimensional detector. The data is scanned vertically to collect the traditional scattering intensity variation with 2θ (which will be shown here as a function of q since different wavelengths were used). The data was also scanned horizontally in order to measure the crystallite misorientation. Since the WAXS detector was not perpendicular to the X-ray beam, the geometry of the pattern is complicated, and will only be presented here in terms of a width in pixels, instead of degrees as can be found for the small-angle orientation angle.

3.3.1. Orientation from WAXS

Fig. 8 shows the change in the orientation of the intense cellulose (200) peak as a sample of dry flax is stretched. The change in intensity is discussed later. It is clear in Fig. 8 that there is a very slight rotation of the crystallites as the sample is stretched, followed by a larger change after it snaps as indicated by the change in peak position. The sudden change after snapping can be attributed to the fibre falling out of the beam to a certain extent. The reorientation before snapping is really limited to the first data frame, suggesting that there is a take-up of stress in the fibre resulting in a very slight crystal rotation.

Although slight rotation changes have been seen in the wide-angle scattering, but none in the small-angle scattering, these results are not in disagreement. If the number of pixels could be calibrated into degrees, an upper limit for the entire width of the detector (512 pixels) would be maybe 90°. The shift of the WAXS peak is ∼5 pixels, giving a maximum total shift of $5 \times 90/512 \sim 0.9°$, less than the accuracy of the SAXS data.

3.3.2. Strain-induced crystallisation

As shown in Fig. 9 the intensity from the wide-angle data increases until the sample breaks, and then starts to decrease again. We have attributed this initial increase in intensity to strain-induced crystallisation of the cellulose chains for a number of reasons:

1. The two-dimensional images were normalised (as discussed in the experimental section), and so the change in intensity is due to some change in the flax fibre and not due to a change in beam intensity.
2. Since the fibres were initially in a taut state it is unlikely that the fibres could have been stretched so that more material was in the beam. Although good

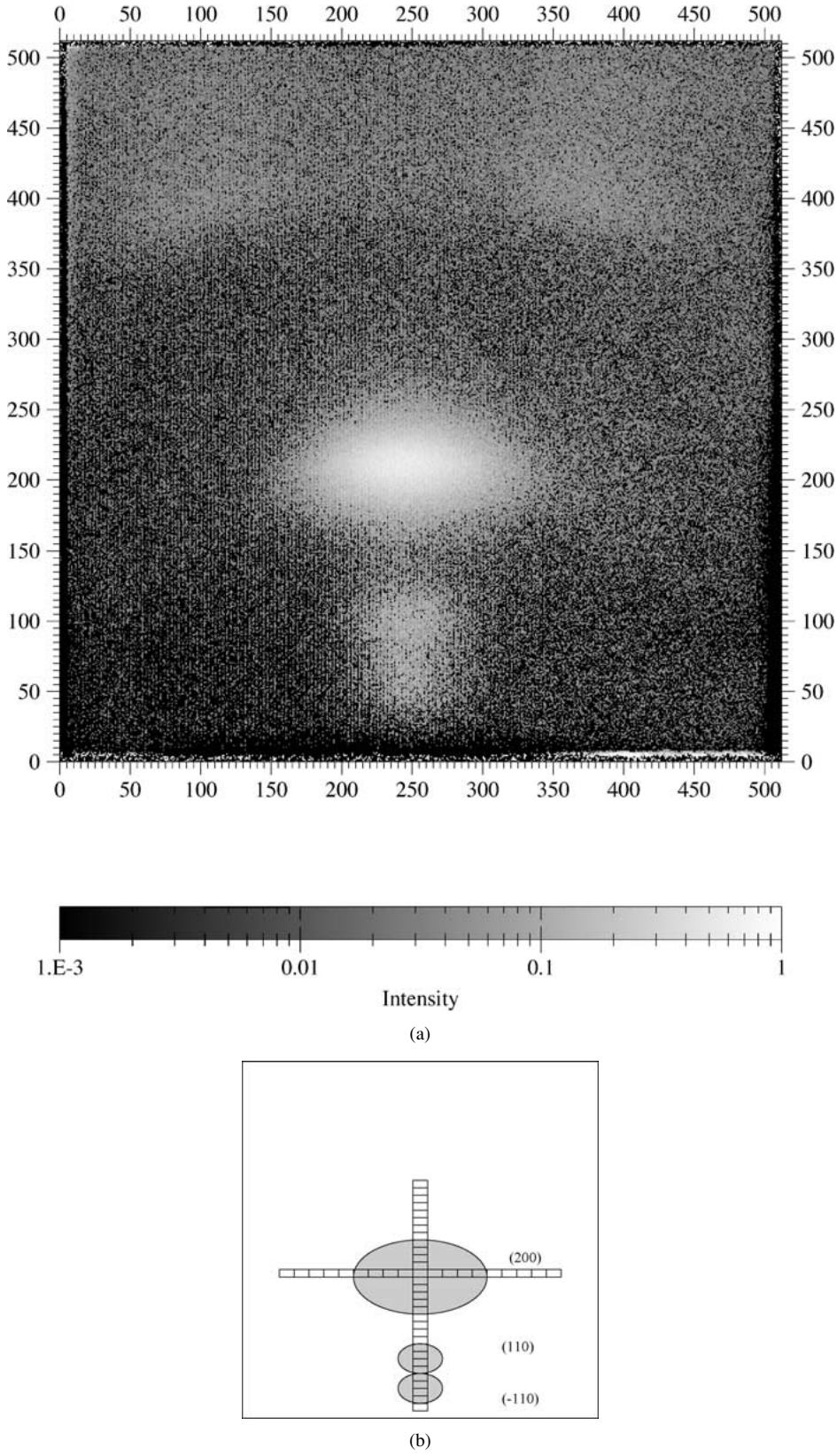

Figure 7 (a) A typical wide-angle diffraction pattern from horizontal flax fibres. (b) A schematic two-dimensional wide-angle scattering pattern from flax fibres, showing how the data is taken from the detector to collect the conventional scattering profile (scan vertically) or the crystal misorientation (scan horizontally). The crystal notation is that of Woodcock and Sarko [24].

simultaneous data does not exist for this experiment, the small-angle data does not show a change in intensity during stretching, and this provides further evidence that the change in the wide-angle data is a real change in structure.

3. After failure the drop in intensity can be interpreted either as the sample falling out of the beam or as relaxation of the molecules. On the basis of the wide-angle data it is not possible to differentiate between these two theories. However small-angle data sometimes also shows a drop in intensity after snapping which would agree with the idea of the sample dropping out of the beam, since small-angle scattering is not sensitive to the crystalline components of the fibre.

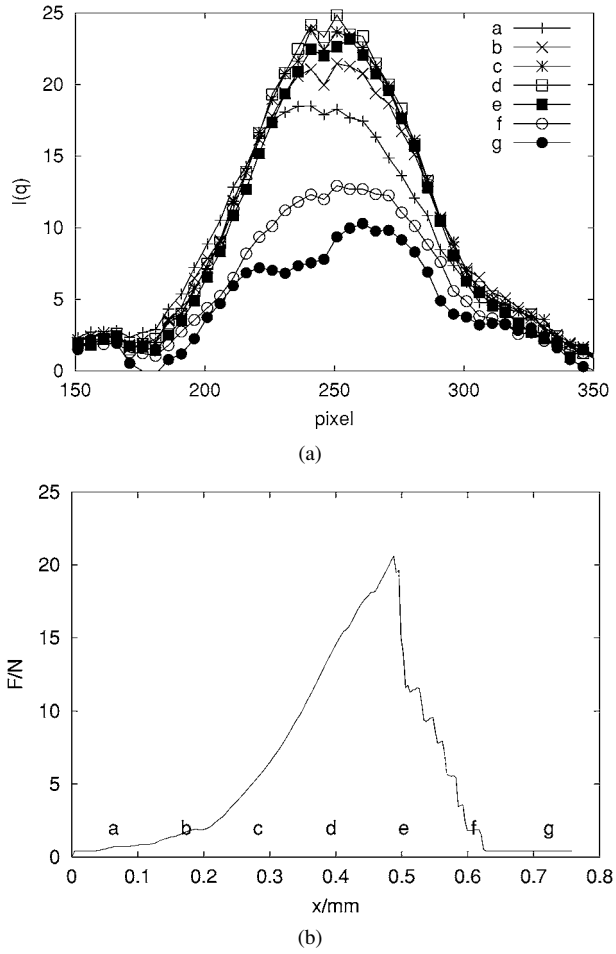

Figure 8 The orientation of the (200) peak of cellulose crystals as dry flax is stretched at 0.011 mm/min. (a) The orientation distribution, found by recording the intensity across the wide-angle detector. Every 5th data point has been plotted to simplify the graph. (b) The load-extension curve. Sample initial length 30 mm.

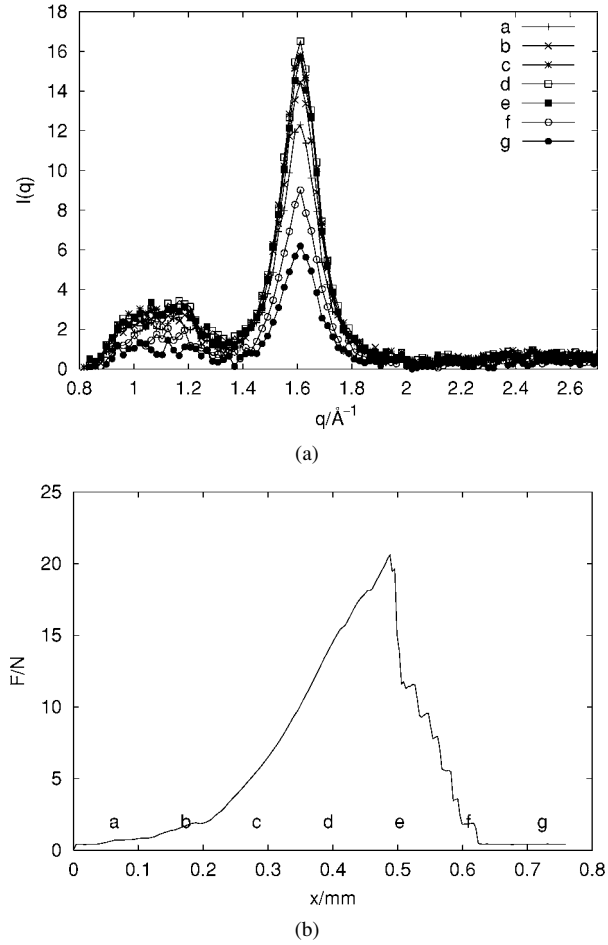

Figure 9 The WAXS scattering curves as a sample of dry flax is stretched at 0.011 mm/min. (a) The WAXS patterns, found by recording the intensity up the wide-angle detector. Every 5th data point has been plotted to simplify the graph. (b) The load-extension curve. Sample initial length 30 mm.

Strain-induced crystallisation is sometimes seen when an initially amorphous polymer film is stretched, causing strain-induced crystallisation once the polymers become oriented [25]. Since the crystallisation shown here starts soon after the sample starts being stretched it can be assumed that the non-crystalline cellulose chains are initially oriented in the same direction as the crystals. This has also been suggested by neutron scattering work [26].

3.4. Comparison with other cellulose systems

We have conducted similar experiments on cellulose produced by the bacteria *Acetobacter xylinum* [27], which has previously been used to model the structure of the primary cell wall [28]. These experiments have shown that the microfibrils from *Acetobacter* are initially isotropic and quickly orientate during deformation to a maximum fwhm of approximately 25°.

This difference between a material supposed to be similar to the primary wall (*Acetobacter*) and one that is almost exclusively secondary wall (flax) is interesting. Although the load-bearing element in each case are cellulose microfibrils, those in *Acetobacter* form only ∼5% of the material (the rest being water), and it is possible that the microfibrils in flax cannot orientate because the system is more dense, and there are more fibril-fibril interactions.

4. Conclusions

To conclude, we have performed small and wide-angle X-ray scattering experiments with *in situ* uniaxial tension on small bundles of flax fibres.

The major result from these experiments was that evidence for strain-induced crystallisation was found. By comparison with other polymer systems it has been concluded that the non-crystalline cellulose chains are initially orientated parallel to the cellulose crystals, and therefore are not truly amorphous.

Otherwise, few changes occur in the flax fibres as they are drawn. Little reorientation of the microfibrils was noticed, and that which did occur was limited to the first part of the extension. No change in the position or in the intensity of the long-period at $q = 0.095$ Å^{-1} (attributed to a non-crystalline/crystalline repeat) was seen, and it has been suggested that this implies that the cellulose chains in the non-crystalline regions are initially taut.

Acknowledgements

We would like to thank M. Butler, C. Moss, M. Sferrazza, C.-P. Ooi, A. Catherall, P. Royall, S. Robinson, J. Sanderson, S. Clarke, and J. Crawshaw

for help with the experiments, and the station managers A. Gleeson, G. Grossmann, and S. Slawson at Daresbury.

We would also like to thank H. Bos of ATO-DLO for supplying the flax fibres, and the BBSRC for funding OMA.

References

1. C. BRETT and K. WALDRON, "Physiology and Biochemistry of Plant Cell Walls" (Unwin Hyman, London, 1990).
2. A. C. O'SULLIVAN, *Cellulose* **4** (1997) 173.
3. M. C. McCANN and K. ROBERTS, in "The Cytoskeletal Basis of Plant Growth and Form," edited by C. W. Lloyd (Academic Press, London, 1991), ch. 9, p. 109.
4. D. J. COSGROVE, *Annu. Rev. Cell. Dev. Biol.* **13** (1997) 171.
5. *Idem*., *Annu. Rev. Plant Physiol. Plant Mol. Biol.* **50** (1999) 391.
6. A. DARVILL, M. McNEIL, P. ALBERSHEIM and D. P. DELMER, in "The Plant Cell," *The Biochemistry of Plants, a Comprehensive Treatise*, Vol. 1, edited by N. E. Tolbert (Academic Press, New York, 1980) ch. 3.
7. O. M. ASTLEY and A. M. DONALD, *Biomacromolecules* (submitted).
8. P. A. RICHMOND, in "Biosynthesis and Biodegradation of Cellulose," edited by C. H. Haigler and P. J. Weimer (Dekker, New York, 1991) ch. 1.
9. D. L. EASSON and R. MOLLOY, *Outlook on Agriculture* **25** (1996) 235.
10. A. N. J. HEYN, *J. Appl. Phys.* **26** (1955) 519.
11. G. C. DAVIES and D. M. BRUCE, *Text. Res. J.* **68** (1998) 623.
12. X.-P. HU and Y.-L. HSIEH, *J. Mater. Sci.* **32** (1997) 3905.
13. M. G. NORTHOLT and H. De VRIES, *Angew. Makromol. Chem.* **133** (1985) 183.
14. M. G. NORTHOLT, J. J. M. BALTUSSEN and B. SCHAFFERS-KORFF, *Polymer* **6** (1995) 3485.
15. M. MÜLLER, C. CZIHAK, G. VOGL, P. FRATZL, H. SCHOBER and C. RIEKEL, *Macromolecules* **31** (1998) 3953.
16. M. SHIOYA and A. TAKAKU, *J. Appl. Phys.* **58** (1985) 4074.
17. O. GLATTER and O. KRATKY, "Small Angle X-ray Scattering" (Academic Press, London, 1982).
18. N. S. MURTHY, K. ZERO and D. T. GRUBB, *Polymer* **38** (1997) 1021.
19. N. S. MURTHY, D. T. GRUBB and K. ZERO, *Macromolecules* **33** (2000) 1012.
20. J. M. SAMON, J. M. SCHULTZ and B. S. HSIAO, *Polymer* **41** (2000) 2169.
21. J. WU, J. M. SCHULTZ, F. YEH, B. S. HSIAO and B. CHU, *Macromolecules* **33** (2000) 1765.
22. N. STRIBECK, D. SAPOUNDJIEVA, Z. DENCHEV, A. A. APOSTOLOV, H. G. ZACHMANN, M. STAMM and S. FAKIROV, *ibid.* **30** (1997) 1329.
23. S. KUMAR, S. WARNER, D. T. GRUBB and W. W. ADAMS, *Polymer* **35** (1994) 5408.
24. C. WOODCOCK and A. SARKO, *Macromolecules* **13** (1980) 1183.
25. G. ALLEGRA and M. BRUZZONE, *Macromolecules* **16** (1983) 1167.
26. M. MÜLLER, C. CZIHAK, H. SCHOBER, Y. NISHIYAMA and G. VOGL, *ibid.* **33** (2000) 1834.
27. O. M. ASTLEY, Ph.D. thesis, University of Cambridge, 2000.
28. S. E. C. WHITNEY, J. E. BRIGHAM, A. H. DARKE, J. S. G. REID and M. J. GIDLEY, *Plant J.* **8** (1995) 491.
29. W. RULAND, *J. Polym. Sci. C* **28** (1969) 143.
30. A. F. THÜNEMANN and W. RULAND, *Macromolecules* **33** (2000) 1848.
31. A. MAHENDRASINGAM, C. MARTIN, W. FULLER, D. J. BLUNDELL, R. J. OLDMAN, D. H. MACKERRON, J. L. HARVIE and C. RIEKEL, *Polymer* **41** (2000) 1217.
32. S. TOKI, T. FUJIMAKI and M. OKUYAMA, *ibid.* **41** (2000) 5423.
33. A. M. HEALEY, P. J. HENDRA and Y. D. WEST, *ibid.* **37** (1996) 4009.
34. P.-H. SING and S.-Y. WU, *ibid.* **39** (1998) 7033.
35. K. P. BATTJES, C.-M. KUO, R. L. MILLER and J. C. SAAM, *ibid.* **28** (1995) 790.
36. M. E. VICKERS, in "Scattering Methods in Polymer Science," edited by R. W. Richards (Ellis Horwood, New York, 1995) ch. 5, p. 103.

Received 19 December 2000
and accepted 26 August 2002